



ELSEVIER

Journal of Hydrology 204 (1998) 150–167

Journal  
of  
**Hydrology**

# Transformation of point rainfall to areal rainfall: Intensity-duration-frequency curves

Murugesu Sivapalan<sup>\*,1</sup>, Günter Blöschl

*Institut für Hydraulik, Gewässerkunde und Wasserwirtschaft, Technische Universität Wien, Karlsplatz 13/223, A-1040 Vienna, Austria*

Received 5 July 1997; revised 16 July 1997; accepted 22 September 1997

## Abstract

Current approaches to constructing catchment intensity-duration-frequency (IDF) curves are dominated by the use of empirically-derived areal reduction factors (ARFs). In this paper we present an alternative methodology which is based on the spatial correlation structure of rainfall. It represents an attempt to link current scientific theories of space-time rainfall fields with design methods. The starting point is to derive the parent distribution of catchment average rainfall intensity from that of point rainfall intensity. The parameters of the two parent distributions are related through a variance reduction factor which is a function of the spatial correlation structure of rainfall and catchment area. Assuming that the parent distribution is of the 'exponential type', it is then transformed to an extreme value distribution of the Gumbel type. The crucial step is to match the parameters of the extreme rainfall distribution derived above, for the particular case of zero catchment area, with those of empirical point IDF curves which have also been fitted to the Gumbel distribution. With this match, the proposed theory then naturally generalises to yield catchment IDF curves for catchments of any size, and for rainfall of any spatial correlation structure. The new catchment IDF curves have the attractive property that, with a minimum number of assumptions, they can reproduce a range of observed properties of catchment rainfall. For example, not only the mean and the standard deviation of extreme rainfall, but also its coefficient of variation, decrease with increasing catchment area. We also find that computed ARFs using the new approach depend not only on catchment area and storm duration, but also on the return period. We estimate ARFs using the new methodology for two major observed storms in Austria, and find that these estimates compare favourably with our understanding of the rainfall generating mechanisms associated with these two particular storm types. © 1998 Elsevier Science B.V.

*Keywords:* Rainfall fields; Flood estimation; Areal reduction factors; Extreme value distributions; Catchments; IDF curves

## 1. Introduction

Intensity-duration-frequency (IDF) curves are widely used in flood design estimation. IDF curves are essentially conditional cumulative distributions

of rainfall intensity, conditioned on rainfall duration. They are estimated from observed rainfall data by sub-dividing the rainfall record into intervals of a given duration. Annual maxima of average rainfall intensities over each of the selected intervals can then be ranked. Based on these rankings one can then calculate, using plotting position formulae, the conditional return period  $T$  corresponding to each value of intensity (the average number of years between rainfall events, of the chosen duration, that

\* Corresponding author.

<sup>1</sup> On leave from: Centre for Water Research, Department of Environmental Engineering, The University of Western Australia, Nedlands, W.A. 6907, Australia.

equal or exceed the particular intensity). For definitions, see Eagleson (1970) and Chow et al. (1988).

The reciprocal of  $T$  is the conditional probability  $P$  that the annual maximum rainfall intensity for a specified duration (averaged over the duration), will equal or exceed a specified magnitude; this can be written as:

$$P\{I \geq i_e | t_r\} = \frac{1}{T} = 1 - \int_0^{i_e} f_i(i | t_r) di = 1 - F_I(i_e | t_r) \quad (1)$$

$F_I(i_e | t_r)$  in Eq. (1) is the conditional cumulative distribution function for intensity  $i_e$ , given duration  $t_r$ , which is a formal expression of the IDF curves. The IDF curves, as mentioned already, are usually based on time increments, rather than on complete storms (Eagleson, 1970; Chow et al., 1988). Gutknecht (1977) investigated the differences between storm-based and increment-based IDF curves using Austrian data. He concluded that, in general, storm-based analyses give lower rainfall intensities for a given duration and return period; however, the differences are small.

### 1.1. Catchment IDF curves and areal reduction factors

The IDF curves described above apply to point rainfall. However, what is needed for most design applications are catchment IDF curves. Due to the smoothing associated with the spatial averaging of rainfall over the catchment area, the catchment IDF curves have both a lower mean and variance, i.e. they are lower and flatter in appearance, than the corresponding point IDF curves.

Current practice for constructing catchment IDF curves is dominated by the use of areal reduction factors (ARFs) which are empirically-derived functions of catchment area,  $A$ , storm duration,  $t_r$ , and sometimes, the return period,  $T$  (U.S. Weather Bureau, 1957; Bell, 1976; Myers and Zehr, 1980; Pilgrim, 1987; Omolayo, 1993; Grebner, 1995; Srikanthan, 1995). Catchment IDF curves are then obtained by multiplying the rainfall intensities estimated from the point IDF curves by the ARF corresponding to  $A$ ,  $t_r$  and  $T$ . For very small catchments the ARF approaches one, and catchment IDF curves become identical to point IDF curves. With increasing catchment area,  $A$ , the ARFs fall away from unity, and

catchment IDF curves become lower and flatter since both the mean and standard deviation of the conditional rainfall distributions are proportionately reduced due to the multiplication by the ARFs. This reduction is much sharper for short duration events, the rationale being that short duration events (e.g. convective) are small in areal extent.

Two kinds of ARFs are presently in use (Eagleson, 1970; Blöschl and Sivapalan, 1995; Srikanthan, 1995). (a) Fixed-area (also known as geographically-fixed) ARFs relate rainfall at any arbitrary point, i.e. a point rainfall estimate, to the average over a catchment which is fixed in space. They are estimated by constructing from all available station rainfall data, the time series of catchment average rainfall (e.g. using the Thiessen polygon method), performing the same types of extreme value analyses described above for constructing point IDF curves, and finally relating the catchment rainfall intensities to the point values, for the same return period and duration. (b) Storm-centred ARFs refer to a given storm. They represent the ratio of average storm depth over an area (defined by the rainfall isohyets) and the maximum rainfall depth for the storm (at the storm centre). Storm-centred ARFs are usually somewhat smaller than fixed-area ARFs. Storm-centred ARFs are used more commonly in PMF (probable maximum flood) estimation, while the fixed-area ARFs are used for designing hydraulic structures for flood control, e.g. bridges and culverts. This paper is concerned with estimating fixed-area ARFs.

Research on rainfall processes in the past 15–20 yr has been dominated by the stochastic modelling of rainfall fields in space and time (e.g. Waymire et al., 1984; Sivapalan and Wood, 1987), a comprehensive review of which has been provided by Foufoula-Georgiou and Georgakakos (1991). These models are based on the space–time correlation structure of rainfall which reflects the conceptual, hierarchical features observed in actual rain systems, such as, cells, cell clusters and rain bands (Austin and Houze, 1972; Hobbs and Locatelli, 1978; Zawadzki, 1973). As such, they are capable of describing different storm types and rainfall generating mechanisms, be they small convective events or large synoptic events. However, these models are rarely used in design.

One notable example of research into ARFs which did use the spatial correlation structure of rainfall

fields is that of Rodríguez-Iturbe and Mejia (1974). In their work, they approximated the rainfall field as a zero mean Gaussian process, and averaged it over a catchment area. The averaging resulted in variance reduction factors which were a function of the assumed spatial correlation structure, and the size and shape of the catchment area. Rodríguez-Iturbe and Mejia (1974) argued that these variance reduction factors could be interpreted as ARFs. However, these ARFs can only refer to parent rainfall intensities and not to extreme rainfalls; indeed, it is not clear what the relevance of these ARFs is to extreme rainfalls. Specifically, in their method, the mean of the areally averaged rainfall does not change with the averaging area which seems more appropriate to the parent process rather than to the extreme value process.

What is needed, therefore, is an extension of the work of Rodríguez-Iturbe and Mejia (1974) that makes use of the spatial correlation structure while looking at the extreme value distributions rather than the parent distributions only. This is being attempted in this paper. The study of rainfall fields has expanded in the last decade, and alternatives to the use of space–time correlation structures are being investigated, such as fractals and multiplicative cascades. For a detailed exposition of recent advances, refer to a recent issue of *Journal of Geophysical Research* (Vol. 101, D21, pp. 26261–26538, 1996; special section on *Space–Time Variability and Dynamics of Rainfall*). These advances may lead to alternative methods for estimating ARFs. Also, Bacchi and Ranzi (1996) have recently proposed another theoretical methodology for estimating ARFs based on crossing properties of high intensity rainfall.

### 1.2. Aim of this paper

In this paper we present a methodology for estimating catchment IDF curves which utilises the spatial correlation structure of rainfall. The paper thus represents an attempt to link approaches used presently in design, based largely on the use of empirically-derived ARFs, with approaches based on some current scientific theories of space–time rainfall fields. In this way we hope to place the estimation of design ARFs on a sounder scientific basis, and at the same time, provide some guidance for new research strategies.

The methodology proposed in this paper consists of four steps. In the first step, we specify a parent distribution of the point rainfall process. In the second step, this point process is averaged over a catchment area. In the third step, we transform the parent distribution of the areally averaged rainfall process to the corresponding extreme value distribution, using the asymptotic extreme value theory of Gumbel (1958). In the fourth and final step, we match the extreme value distribution derived above, for the particular case of zero catchment area, with observed extreme value distributions of point rainfall (i.e. point IDF curves), which then yield the parameters of the catchment IDF curves. These steps are described in more detail in the following sections, and applications of the methodology are given at the end of the paper.

## 2. Point rainfall—parent distribution

The probability distribution of point rainfall intensities has been examined in a large number of studies (e.g. Eagleson, 1972; Warrilow et al., 1986). In many cases the exponential distribution has been suggested as presenting a good approximation to the underlying rainfall process. For this reason, and for clarity of presentation, we assume that the parent distribution of point rainfall intensity,  $i_p$ , is exponential, with parameter  $\beta_p$ :

$$f_I(i_p) = \frac{1}{\beta_p} \exp\left(-\frac{i_p}{\beta_p}\right) \quad (2)$$

with its mean and variance given by:

$$\mu_p = \beta_p \quad (3)$$

$$\sigma_p^2 = \beta_p^2 \quad (4)$$

However, the methodology presented here can be easily extended to any other distribution belonging to the ‘exponential’ type (see Gumbel, 1958), such as, the Weibull and gamma distributions.

It is also common to assume that the spatial correlogram, of point rainfall intensity, is of the following isotropic, exponential type (Rodríguez-Iturbe and Mejia, 1974; Wood and Hebson, 1986):

$$\rho_p(r) = \exp(-r/\lambda) \quad (5)$$

where  $r$  is the distance between two points and  $\lambda$  is

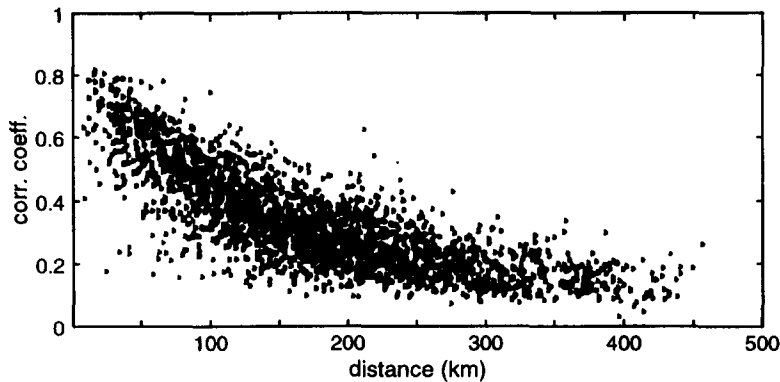


Fig. 1. Spatial correlation coefficients (i.e., the correlogram) versus inter-station distance based on daily rainfall data at 67 stations in Tunisia during 1979–1983 (after Berndtsson, 1988).

the spatial correlation length defined by

$$\lambda = \int_0^\infty \rho_p(r) dr$$

For illustration, and to support the assumption of an exponential correlogram, we present in Fig. 1(a) the spatial correlogram, copied from Berndtsson (1988), based on daily rainfall data obtained from 67 stations in Tunisia for the 5 yr period 1979–1983.

Again, although we have adopted an isotropic, exponential correlogram here for clarity of presentation, the proposed methodology can be easily generalised for any other correlation structure, as well as for anisotropic conditions. For example, Sivapalan et al. (1990) have used a nested spatial correlogram (a combination of two different correlation lengths) of the double-exponential type, while Blöschl and Sivapalan (1997b) have used a nested correlogram of the exponential type.

### 3. Areal averaging of parent distribution

#### 3.1. Effects of areal averaging

Assuming that the spatial random field of point rainfall intensities is stationary, we are now interested in how the spatial moments change due to the averaging by a catchment of area  $A$ . The spatially averaged (over the area  $A$ ) rainfall intensity  $i_A$  is defined as:

$$i_A = \frac{1}{A} \int_A i_p(\mathbf{x}) d\mathbf{x} \tag{6}$$

where  $\mathbf{x}$  is a vector representing the coordinates of an arbitrary point inside the area. Because of stationarity the mean of  $i_A$  remains the same as that of  $i_p$ . That is:

$$\mu_A = \mu_p \tag{7}$$

The variance of the areally averaged process,  $\sigma_A^2$ , is less than  $\sigma_p^2$ , with the ratio  $\sigma_A^2/\sigma_p^2$  usually called the variance reduction factor, denoted by  $\kappa^2$ . That is:

$$\sigma_A^2 = \sigma_p^2 \kappa^2 \tag{8}$$

The variance reduction factor  $\kappa^2$  decreases with increasing  $A$ ;  $\kappa^2 = 1.0$  when  $A = 0$ , and  $\kappa^2 \rightarrow 0$  as  $A \rightarrow \infty$ .

#### 3.2. Estimation of $\kappa^2$

The magnitude of the variance reduction factor  $\kappa^2$  depends on the correlation structure of rainfall, and the size and shape of the catchment. Rodríguez-Iturbe and Mejía (1974) showed that  $\kappa^2$  can be expressed for a stationary isotropic spatial random field as:

$$\kappa^2 = E[\rho_p(|\mathbf{x}_2 - \mathbf{x}_1|)] \tag{9}$$

where  $E[\rho_p]$  is the expected value of the spatial correlation coefficient between any two points  $\mathbf{x}_1$  and  $\mathbf{x}_2$  randomly chosen within a catchment domain of size  $A$ , and  $|\cdot|$  represents the magnitude of the Euclidean distance between them. Rodríguez-Iturbe and Mejía (1974) also showed that Eq. (9) can be simplified to:

$$\kappa^2 = \int_0^{R_{\max}} \rho_p(r) f_R(r) dr \tag{10}$$

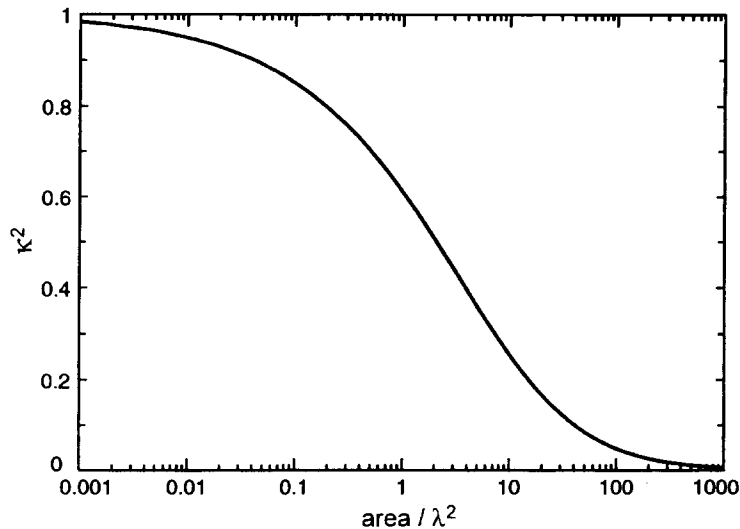


Fig. 2. Variance reduction factor  $\kappa^2$  versus nondimensional catchment area,  $A/\lambda^2$ . The catchment area is approximated by a square and the correlogram is exponential.

where  $R = r$  is the Euclidean distance between any two points within the area,  $R_{\max}$  is the maxima of  $r$  for all pairs of points within the area, and  $f_R(r)$  is the pdf of the random variable  $R = r$ .

In this paper we have assumed the catchment to be a square of side  $a$ , i.e.  $A = a^2$ ; the pdf of  $R$  has been derived by Ghosh (1951) for this case, and is reproduced in Appendix A. Using Eq. (10) we have estimated  $\kappa^2$  for a range of catchment sizes,  $A$ , for the case of a square shaped catchment and the isotropic, exponential correlogram given by Eq. (5). The results are presented in Fig. 2 in dimensionless form as  $\kappa^2$  versus  $A/\lambda^2$ . Note that  $\kappa^2$  presented in Fig. 2 is identical to the variance reduction factor presented by Rodríguez-Iturbe and Mejía (1974) in their Figure 5.

We want to reiterate that the methodology presented here is not limited by the assumptions of isotropy and square shape of the catchment area. These can easily be generalised. For example, the distribution,  $f_R(r)$ , of distances can be analytically derived for a rectangle (Ghosh, 1951), and numerically for any other catchment shape (Rodríguez-Iturbe and Mejía, 1974; Sivapalan et al., 1996). Similarly, the methodology can be generalised to relax the assumption of isotropy (see, for example, Sivapalan, 1986); isotropy is only adopted here for clarity of presentation.

However, the assumption of stationarity in space of the underlying rainfall random field is crucial to the derivations presented here. For example, this approach cannot handle finiteness of storm area, and the consequent, possibly partial coverage of a catchment area. At best, the method could be appropriate for rainfall systems which are large relative to catchment area. There have been some studies of the effect of partial coverage of storms; see, for example, Eagleson and Qinliang (1985).

### 3.3. Parent distribution of areal average rainfall

It can be shown that, when the point rainfall process is exponentially distributed, the areally averaged rainfall process is approximately gamma distributed (Hebson and Wood, 1986; Wood and Hebson, 1986; Sivapalan et al., 1990). We adopt the following gamma distribution, with parameters  $k_A$  and  $\beta_A$ , as the parent distribution of areal average rainfall:

$$f_I(i_A) = \left(\frac{i_A}{\beta_A}\right)^{k_A} \exp\left(-\frac{i_A}{\beta_A}\right) / \beta_A \Gamma(k_A) \quad (11)$$

The mean and variance for the gamma distribution

are given by:

$$\mu_A = k_A \beta_A \tag{12}$$

$$\sigma_A^2 = k_A \beta_A^2 \tag{13}$$

Using Eqs. (3) and (4) and Eqs. (7) and (8), we then have:

$$k_A \beta_A = \beta_p \tag{14}$$

$$k_A \beta_A^2 = \beta_p^2 \kappa^2 \tag{15}$$

where  $\kappa^2$  is the variance reduction factor estimated with Eq. (10). From Eqs. (14) and (15) we can then solve for  $k_A$  and  $\beta_A$  as follows:

$$k_A = \kappa^{-2} \tag{16}$$

$$\beta_A = \beta_p \kappa^2 \tag{17}$$

Eqs. (16) and (17) therefore describe how the parameters of the parent distribution of areally-averaged rainfall change with catchment area  $A$ .

**4. Areal rainfall: Transition to extreme values**

In this paper we are concerned with obtaining the distribution of extreme rainfall, i.e. the largest value in a single calendar year. Gumbel (1958) (also see

Benjamin and Cornell, 1970, pp. 670–672), considered random variables, denoted by  $X$ , with underlying parent distributions of the ‘exponential’ type, and the distribution  $F_{Y_n}$  of  $Y_n$ , the largest of  $n$  independent, identically distributed random variables  $X_1, X_2, X_3, \dots, X_n$  sampled from  $F_X(x)$ . An ‘exponential’ type distribution is one whose cumulative distribution, in the upper tail only, can be written in the form:

$$F_X(x) = 1 - \exp[-g(x)] \tag{18}$$

with  $g(x)$  an increasing function of  $x$ . The gamma distribution assumed earlier for areal average rainfall is of this type, as is, naturally, the exponential distribution itself. Gumbel (1958) then showed that the distribution of  $Y_n$ , the largest of  $n$  independent random variables drawn from  $F_X(x)$  is given by:

$$F_{Y_n}(y) = \exp\{-\exp[-\alpha_n(y - u_n)]\} \tag{19}$$

where  $\alpha_n$  and  $u_n$  are parameters of a linear approximation to  $g(x)$  for large (i.e. extreme) values of  $x$ . This approximation is given by:

$$g(x) \approx g(u_n) + \alpha_n(x - u_n) \tag{20}$$

The upper tail is defined, following Gumbel (1958), as that corresponding to any chosen value of  $n$ , i.e.

$$u_n = g^{-1}(\ln n) \tag{21}$$

where  $u_n$  is the rainfall intensity beyond which we fit

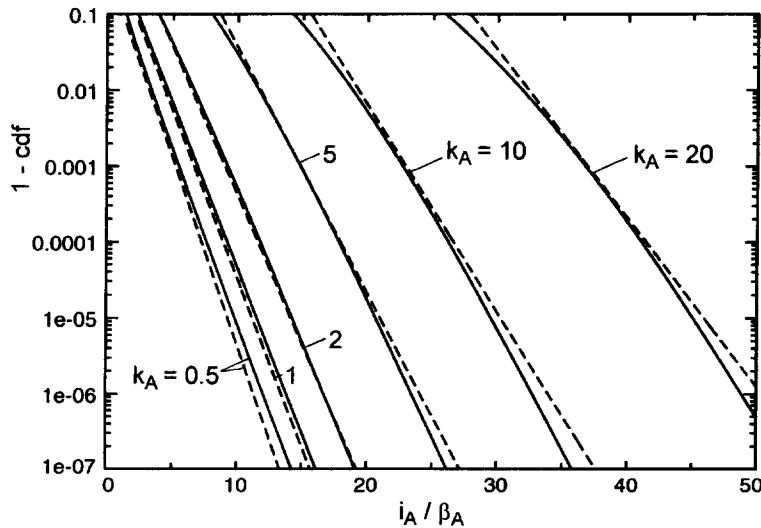


Fig. 3. Best fits to  $1 - F_I(i_A)$  for the gamma distribution of areally averaged rainfall intensity for different values of the parameters  $k_A$  and  $\beta_A$ . Solid lines are exact and dashed lines correspond to approximate expressions adopted in this paper (Eqs. (22)–(26)).

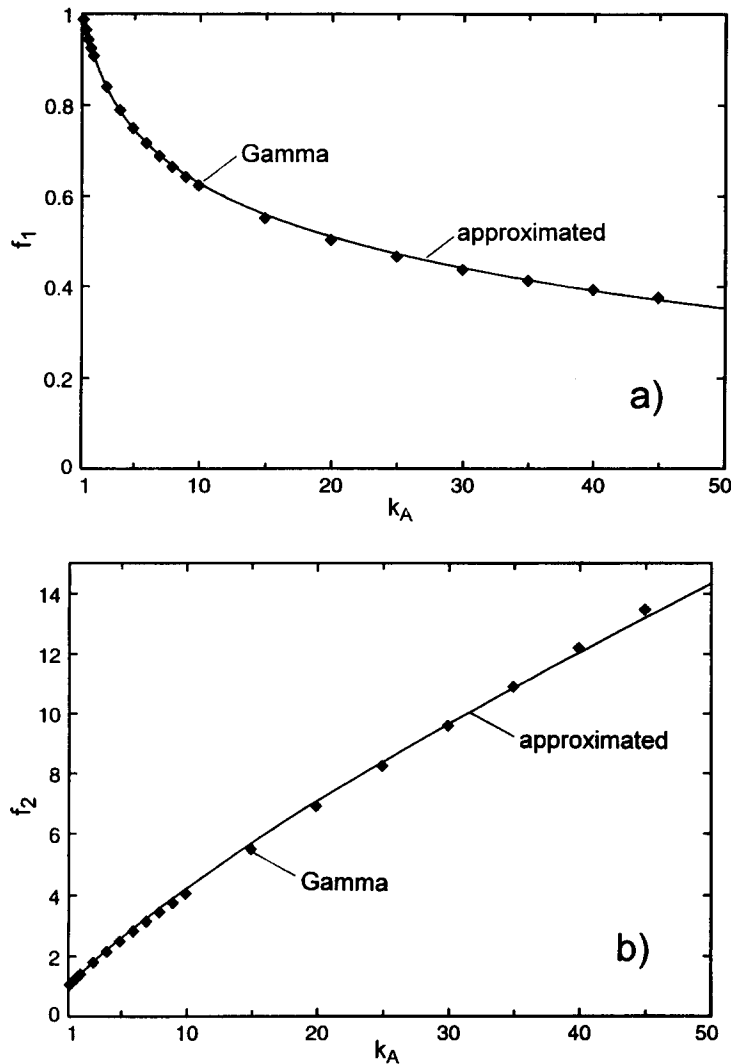


Fig. 4. Fitted functions  $f_1(k_A)$  and  $f_2(k_A)$  as functions of the gamma parameter  $k_A$ .

the tail of the parent distribution with Eqs. (18) and (20), and  $n$  can be interpreted as the reciprocal of the probability that this intensity is exceeded in any rainfall event.

We constructed the cumulative parent distribution function,  $F_I(i_A)$ , for areal average rainfall intensities which are gamma distributed, with the pdf given by Eq. (11) with parameters  $k_A$  and  $\beta_A$ . We fitted the upper tail of this cumulative distribution, more specifically that part of the distribution for which  $1 - F_I(i_A) \leq 0.01$  (corresponding to  $n = 100$ ), to an

exponential function of the type:

$$1 - F_I(i_A) \approx \exp\{-[g(u_{nA}) + \alpha_{nA}(i_A - u_{nA})]\} \quad (22)$$

The best fits of the approximate exponential function to  $1 - F_I(i_A)$  are presented in Fig. 3, for different values of the gamma parameters  $k_A$  and  $\beta_A$ . Both the slope,  $\alpha_{nA}$ , and the intercept,  $u_{nA}$ , are functions of parameters  $k_A$  and  $\beta_A$ . Based on fits for a large number of values of  $k_A$  we obtained functional forms for slope and intercept of the following

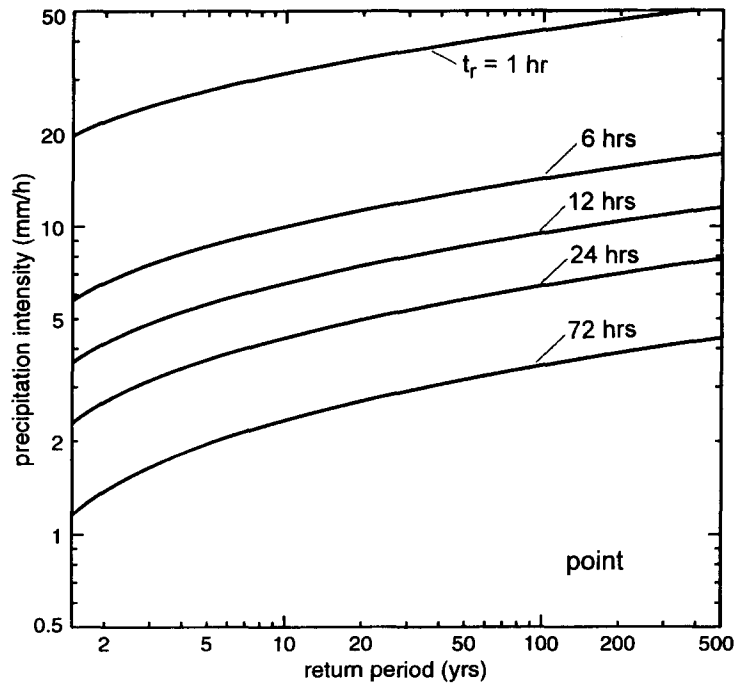


Fig. 5. Point IDF curves for rainfall regime represented by K-45 stations in Austria (after Schimpf, 1970; Sivapalan et al., 1997).

type:

$$\alpha_{nA} = f_1(k_A) / \beta_A \tag{23}$$

$$u_{nA} = f_2(k_A) \beta_A \ln n \tag{24}$$

The functional forms  $f_1(k_A)$  and  $f_2(k_A)$  were obtained empirically, and are presented in Fig. 4(a) and (b), respectively. The fitted relationships for  $f_1(k_A)$  and  $f_2(k_A)$  are as follows:

$$f_1(k_A) = 1 - 0.17 \ln k_A \tag{25}$$

$$f_2(k_A) = 0.39 + 0.61 k_A^{0.8} \tag{26}$$

Note that, despite the empirical manner in which Eq. (23) to Eq. (26) were obtained, these are generic properties of the gamma distribution (valid for  $n = 100$ ), applicable to a large range of parameters  $k_A$  and  $\beta_A$ , and thus have wide applicability.  $k_A$  in Eqs. (25) and (26) is related to  $\kappa^2$  through Eq. (16).

**5. Linking point rainfall to areal rainfall: Extreme values**

In the analyses presented above we have fitted the

upper tail of the cumulative distribution of areally averaged parent rainfall, by an ‘exponential’ function with parameters  $\alpha_{nA}$  and  $u_{nA}$  (Eq. (22)). Therefore, through the Gumbel (1958) theory of extremes, these are also the parameters of the Gumbel distribution of areally averaged extreme rainfall intensity (Eq. (19)), which make them also parameters of the catchment IDF curves. Both  $\alpha_{nA}$  and  $u_{nA}$  are functions of  $k_A$  and  $\beta_A$ , and through the dependence of the latter two parameters on  $\kappa^2$ , they are also functions of the scaled catchment area,  $A/\lambda^2$ . This dependence on catchment area allows us to use the relationships derived above to describe how the catchment IDF curves change with catchment area.

However, at this stage  $\alpha_{nA}$  and  $u_{nA}$  remain relative quantities only, with their absolute magnitudes yet to be determined. This is because, while the variance reduction due to the areal averaging of the rainfall field has been incorporated through  $A/\lambda^2$ , the value of  $\beta_p$ , which determines the absolute value of the variance of point rainfall intensities, has not been specified yet. The specification of these absolute values is the crucial point of this paper. We achieve this by matching the above-derived parameters of the

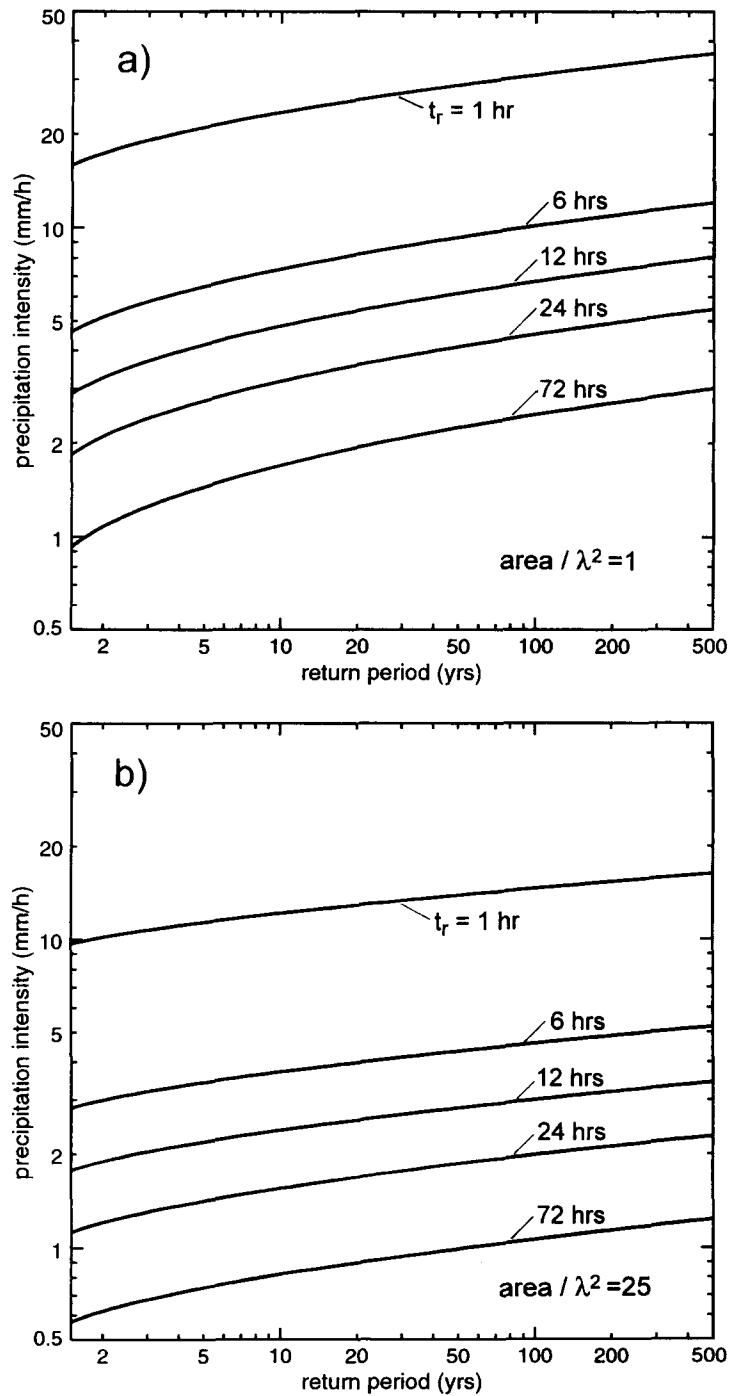


Fig. 6. Catchment IDF curves for rainfall regime represented by K-45 stations in Austria. (a)  $A/\lambda^2 = 1.0$ ; and (b)  $A/\lambda^2 = 25.0$ .  $A$  is the catchment area and  $\lambda$  is the spatial correlation length of rainfall intensities.

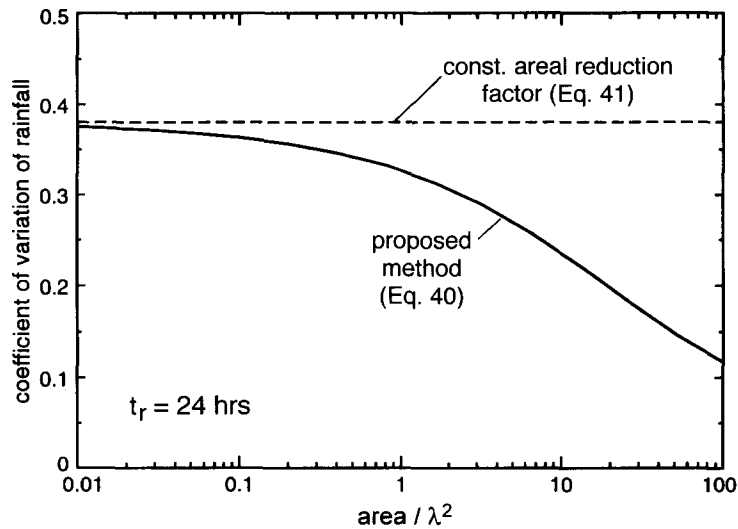


Fig. 7. Coefficient of variation, CV, of catchment extreme rainfall intensities as a function of scaled catchment area  $A/\lambda^2$  estimated by the proposed method (solid line) for the K – 45 regime and  $t_r = 24$  hours. Dashed line represents the constancy of CV associated with an areal reduction factor which does not change with return period.

catchment IDF curves, for the particular case of zero catchment area, i.e.  $A = 0$ , with the parameters of observed, point IDF curves. This match will then yield the required absolute values of the parameters of catchment IDF curves. The procedure for this is formally presented next.

For point rainfall, since the parent distribution is exponential (Eq. (2)), the relationships given by Eqs. (20) and (21) are exact, and the extreme value parameters for point rainfall,  $\alpha_{np}$  and  $u_{np}$ , are given by:

$$\alpha_{np} = 1/\beta_p \tag{27}$$

$$u_{np} = \beta_p \ln n \tag{28}$$

On the other hand, the corresponding (approximate) relationships for areally-averaged rainfall can be obtained from Eqs. (16) and (17) and Eqs. (23) and (24) as follows:

$$\alpha_{nA} = \frac{f_1(\kappa^{-2})}{\kappa^2 \beta_p} \tag{29}$$

$$u_{nA} = f_2(\kappa^{-2}) \beta_p \kappa^2 \ln n \tag{30}$$

The parameters for point and areally-averaged, extreme rainfall can now be compared. Combining

Eq. (27) with Eq. (29) and Eq. (28) with Eq. (30), we obtain:

$$\frac{\alpha_{nA}}{\alpha_{np}} = \frac{f_1(\kappa^{-2})}{\kappa^2} \tag{31}$$

$$\frac{u_{nA}}{u_{np}} = \kappa^2 f_2(\kappa^{-2}) \tag{32}$$

Eqs. (31) and (32) connect the parameters of the probability distribution of point extreme rainfall to those of areal average extreme rainfall. The effects of catchment size and spatial rainfall structure enter Eqs. (31) and (32) through the dependence of the variance reduction factor,  $\kappa^2$ , on  $A/\lambda^2$ .

Note that while the extreme value distribution parameters  $u_{np}$  and  $u_{nA}$  given by Eq. (27) to Eq. (30) are dependent upon the chosen value of  $n$  explicitly, this explicit dependence has been eliminated in the ratios of these parameters given in Eqs. (31) and (32). Nevertheless, there is an implicit dependence of the functions  $f_1(k_A)$  and  $f_2(k_A)$  on the value of  $n$  chosen to approximate the tail of the cumulative gamma distribution; note that the approximations given by Eqs. (25) and (26) were obtained for  $n = 100$ . This implicit dependence of  $f_1(k_A)$  and  $f_2(k_A)$  on  $n$  will only have a relatively minor impact on the results presented in the remainder of this paper.

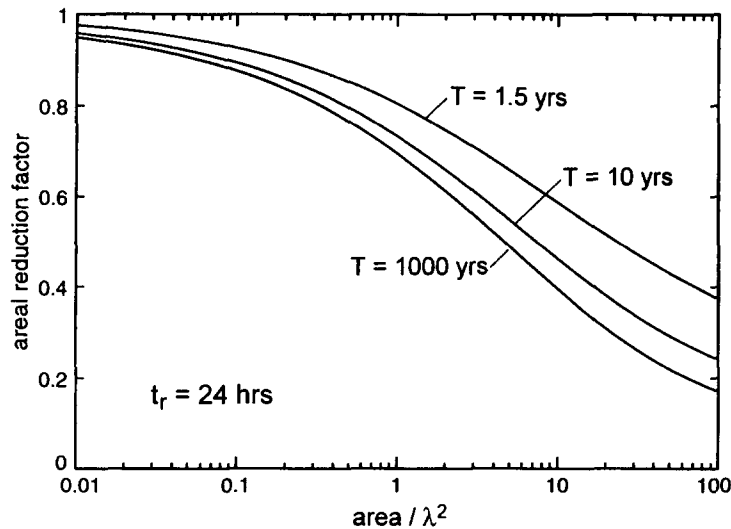


Fig. 8. Areal reduction factors estimated by the proposed method for the K-45 rainfall regime in Austria, for  $t_r = 24$  hours, as functions of scaled catchment area  $A/\lambda^2$  and return period,  $T$ .  $A$  is the catchment area and  $\lambda$  is the spatial correlation length of rainfall.

As shown in previous sections, the derivations using the Gumbel (1958) extreme value theory give rise to a Gumbel (Extreme Value Type I) distribution for catchment average rainfall intensity. The crucial point is that observed point IDF curves, often, are also closely fitted by a Gumbel distribution. If both the observed and derived extreme value distributions (i.e. for point rainfall) are of the Gumbel type, then we can match their parameters.

For illustration, we take the example of the IDF curves for the rainfall regime characterised by ‘K-45 stations’ in Austria; these are shown in Fig. 5 (taken from Schimpf, 1970). Sivapalan et al. (1997) and Blöschl and Sivapalan (1997a) fitted the following conditional cumulative Gumbel distribution to these IDF curves:

$$F_I(i_e|t_r) = \exp\{-\exp[-b(t_r)(i_e - c(t_r))]\} \quad (33)$$

with the parameters  $b$  and  $c$ , which are functions of duration  $t_r$ , being expressed by the following empirical relationships:

$$b(t_r) = -0.05 + 0.25t_r^{0.49} \quad (34)$$

$$c(t_r) = 0.2 + 20.0t_r^{-0.70} \quad (35)$$

Eqs. (34) and (35) apply specifically to the rainfall regime of ‘K-45 stations’ in Austria.

Note the identical form of Eq. (19) and Eq. (33), and in the case of extreme point rainfall, the correspondence between  $b(t_r)$  and  $c(t_r)$  in Eq. (33) and the parameters  $\alpha_{np}$  and  $u_{np}$  in Eqs. (27) and (28), respectively. This correspondence then allows us to replace  $\alpha_{np}$  and  $u_{np}$  in Eqs. (31) and (32), with, respectively,  $b(t_r)$  and  $c(t_r)$  given by Eqs. (34) and (35). In this way, we can then express the parameters  $\alpha_{nA}$  and  $u_{nA}$  in terms of  $b(t_r)$ ,  $c(t_r)$ , and  $\kappa^2$  as follows:

$$\alpha_{nA} = b(t_r) \frac{f_1(\kappa^{-2})}{\kappa^2} \quad (36)$$

$$u_{nA} = c(t_r) \kappa^2 f_2(\kappa^{-2}) \quad (37)$$

Eqs. (36) and (37), in essence, provide the generalised Gumbel parameters for an areally-averaged, extreme rainfall intensity as functions of duration,  $t_r$ , with the effects of catchment area and rainfall correlation structure expressed through  $\kappa^2$ . Note again that the functions  $f_1(k_A)$  and  $f_2(k_A)$  in Eqs. (36) and (37) are generic properties of the gamma distribution (for the chosen value of  $n = 100$ ), while the parameters  $b(t_r)$  and  $c(t_r)$  apply specifically to the Austrian rainfall regime of K-45 stations.

Nevertheless, there is an implicit  $n$  associated with the empirical IDF curves and the associated parameters  $b(t_r)$  and  $c(t_r)$ , just as there is an implicit  $n$  ( $n = 100$ ) associated with the functions  $f_1(k_A)$  and

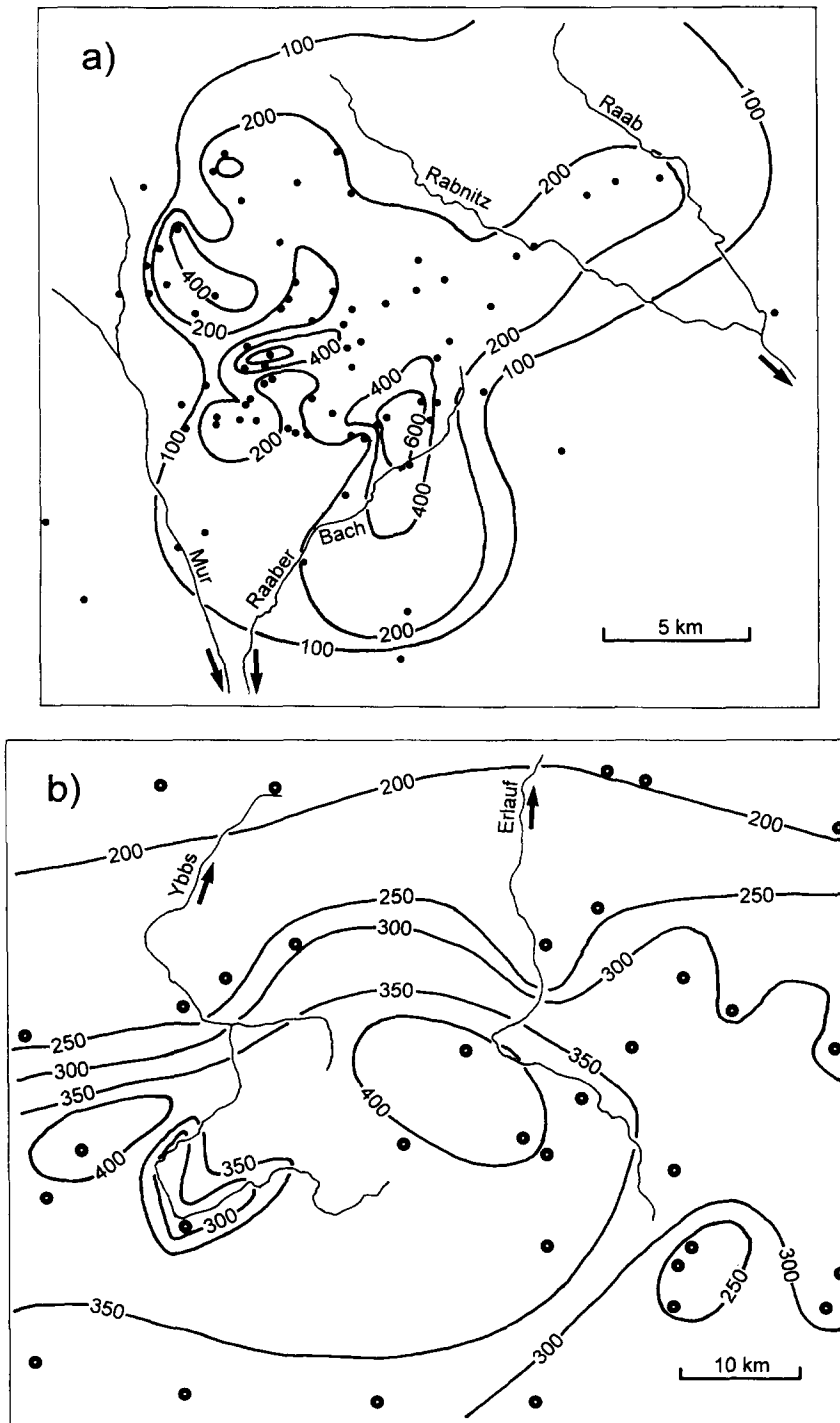


Fig. 9. Isohyetal patterns for two selected storms. (a) Storm on July 16, 1913, in the Stifting region, Styria, Austria and (b) the storm during September 10–13, 1899, in the Erlauf region of Lower Austria. Isohyets are in mm depth units.

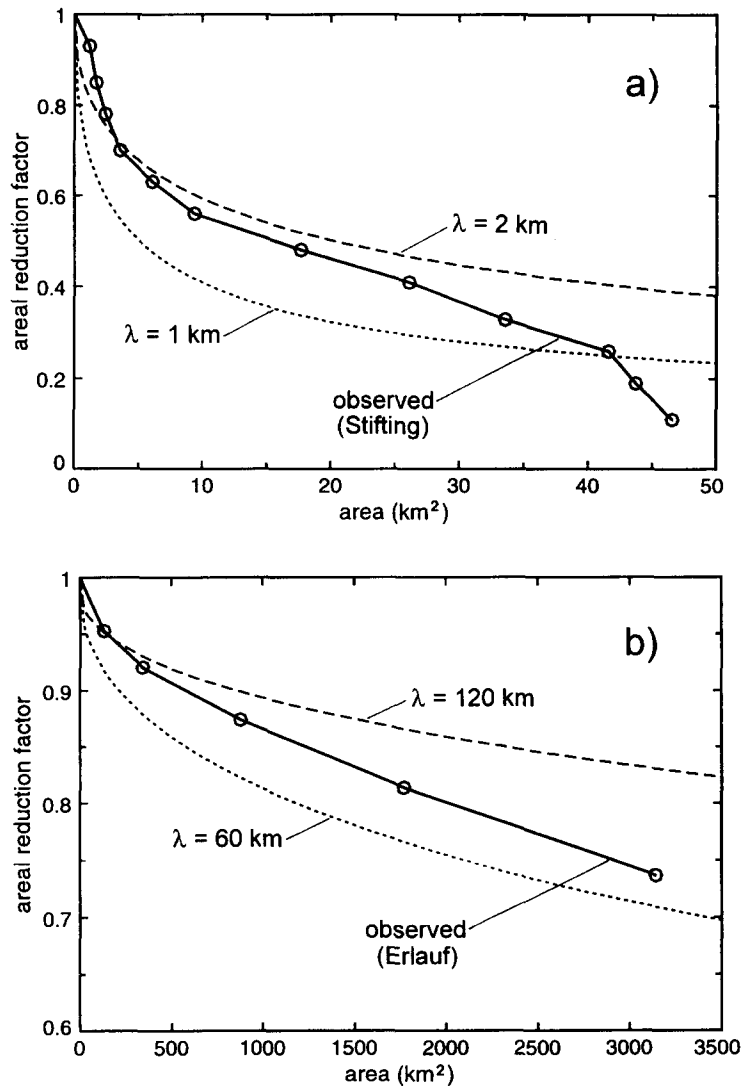


Fig. 10. Empirical areal reduction factors (a) for the July 16 storm of 1913 in the Stifting region, and (b) the September 10–13 storm of 1899 in the Erlauf region, obtained from the isohyetal patterns of Fig. 9 (lines with markers). Areal reduction factors estimated by the proposed method are presented for two enveloping correlation lengths (solid lines).

$f_2(k_A)$ . This difference should be noted even though  $n$  does not appear explicitly in Eqs. (36) and (37). In this regard, it may help to view the role of  $n$ , not merely as specifying the number of storms per year but also as determining the cutoff point which defines the upper tail of the cumulative distribution function of parent rainfall intensity (see Eq. (22)). In other words, the only difference between the empirical and theoretical approaches is in the cutoff point adopted for extremal

analysis. We believe this difference could affect the accuracy of the estimates of  $\alpha_{nA}$  and  $u_{nA}$  marginally; the methodology itself remains valid.

The parameters  $\alpha_{nA}$  and  $u_{nA}$  from Eqs. (36) and (37) can now be used to construct *catchment* IDF curves for catchments of any size,  $A$ . Fig. 6(a) and (b) present, respectively, two sets of catchment IDF curves for two different catchment areas (normalised by the square of the spatial correlation length), i.e.  $A/\lambda^2 = 1.0$

and  $A/\lambda^2 = 25.0$ , constructed using Eqs. (36) and (37) for the rainfall regime represented by K-45 stations in Austria. Both the mean and standard deviation of areally-averaged, extreme rainfall decrease with increasing catchment size, but at different rates. Similar behaviour has been observed in measured extreme rainfall data (e.g. Berndtsson, 1988). This would mean that the coefficient of variation,  $CV$ , of extreme rainfall would not remain constant, but would change with catchment area. This has important ramifications for the behaviour of ARFs, as will be illustrated in the next section. It is also interesting to note in Fig. 6 the decreasing mean with increasing averaging area, which is at variance with the results of Rodríguez-Iturbe and Mejia (1974), whose mean remained constant. This is because their estimates of ARFs only applied to parent rainfall intensities, and not to the corresponding extreme rainfall intensities.

### 6. Application and discussion

In this section we investigate how the theory of catchment IDF curves described above represents two aspects of the scaling behaviour of extreme rainfall distributions, namely, the relationship of the coefficient of variation with catchment area, and the dependence on return period of the ARFs estimated by the proposed methodology.

#### 6.1. Coefficient of variation

Using the properties of the Gumbel distribution (Chow et al., 1988) one can estimate the mean, standard deviation, and coefficient of variation, of extreme rainfall at the catchment scale. The mean and standard deviation are given by:

$$\mu_{eA} = u_{nA} + 0.5772/\alpha_{nA} \tag{38}$$

$$\sigma_{eA} = \frac{\pi}{\sqrt{6}\alpha_{nA}} \tag{39}$$

which, using Eqs. (36) and (37), can be expanded as follows:

$$\mu_{eA} = \kappa^2 \left\{ c(t_r)f_2(\kappa^{-2}) + \frac{0.5772}{b(t_r)f_1(\kappa^{-2})} \right\} \tag{40}$$

$$\sigma_{eA} = \kappa^2 \frac{\pi}{\sqrt{6}b(t_r)f_1(\kappa^{-2})} \tag{41}$$

Eqs. (40) and (41) can then be combined to yield the coefficient of variation:

$$CV_{eA} = \frac{\pi/\sqrt{6}}{0.5772 + b(t_r)c(t_r)f_1(\kappa^{-2})f_2(\kappa^{-2})} \tag{42}$$

For comparison, the coefficient of variation of extreme point rainfall can be derived directly from Eq. (33), or by putting  $\kappa^2 = 1$  in Eq. (42). This gives:

$$CV_{ep} = \frac{\pi/\sqrt{6}}{0.5772 + b(t_r)c(t_r)} \tag{43}$$

Fig. 7 presents the coefficients of variation estimated using Eqs. (42) and (43) for  $t_r = 24$  hours, for the rainfall regime represented by the K-45 stations in Austria. The coefficient of variation,  $CV$ , estimated by the proposed method, decreases with catchment area,  $A$ . This has important ramifications for the type of ARFs produced. Consider an ARF which is assumed independent of the return period. The use of such a constant proportionality factor to multiply the IDF curves (i.e. regardless of return period) changes both the mean and standard deviation of the IDF curves by the same ratio. This means that  $CV$  remains constant, regardless of catchment area. The constant value of  $CV$  in this case would be identical to that of the point IDF curves, which is given by Eq. (43) and shown by the dashed line in Fig. 7. In contrast, the fact the  $CV$  estimated by the proposed method decreases with catchment area clearly suggests that the ARFs that would be estimated by this method are indeed functions of the return period. This is shown later in this section.

One may expect the dependence of the  $CV$  of rainfall intensity on catchment size to be directly related to the  $CV$  behaviour for flood peaks. The adoption of an ARF that is independent of return period (leading to constant rainfall  $CV$ ), appears to match the main assumption behind the index flood method (Dalrymple, 1960; Chow et al., 1988), namely that the  $CV$  of flood peaks are independent of catchment area. However, there is recent evidence which seems to suggest that the  $CV$  of flood peaks in fact decreases with catchment size (Smith, 1992; Gupta and Dawdy, 1995; Blöschl and Sivapalan, 1997b). The  $CV$ s of rainfall, obtained according to the methodology

presented in this paper, are more consistent with the latter finding.

### 6.2. Areal reduction factors

The ARFs associated with the proposed method can be obtained from the equations for the point and catchment IDF curves presented before. First, an expression for extreme point rainfall intensity  $i_e$  can be derived by inverting Eq. (33), and noting that  $F = (T - 1)/T$ . Similarly, an expression for extreme catchment rainfall intensity  $i_{eA}$  can be derived by inverting Eq. (19) for a catchment of area  $A$ , using expressions for  $\alpha_{nA}$  and  $u_{nA}$  from Eqs. (36) and (37). The ARF is defined simply as the ratio  $i_{eA}/i_e$ ; using the expressions derived, and after some simplification, this leads to:

$$ARF[\kappa^2(A/\lambda^2), t_r, T] = \frac{b(t_r)c(t_r)\kappa^2 f_2(\kappa^{-2}) - \frac{\kappa^2}{f_1(\kappa^{-2})} \ln \left\{ \ln \left( \frac{T}{T-1} \right) \right\}}{b(t_r)c(t_r) - \ln \left\{ \ln \left( \frac{T}{T-1} \right) \right\}} \quad (44)$$

Eq. (44) clearly demonstrates that the ARF depends on catchment area,  $A$ , spatial correlation length,  $\lambda$ , duration,  $t_r$ , and the return period,  $T$ . Fig. 8 presents the ARFs estimated in this way for three different return periods ( $T = 1.5$  yr, 10 yr, and 1000 yr) for the case of  $t_r = 24$  h. It shows, in particular, that the ARF decreases both with increasing catchment size and with increasing return period; this is consistent with observations (Blöschl et al., 1995; Myers and Zehr, 1980; Srikanthan, 1995).

It is also interesting to examine the ARF for very large return periods. For  $T \rightarrow \infty$ , Eq. (44) becomes:

$$ARF[\kappa^2(A/\lambda^2)] = \frac{\kappa^2}{f_1(\kappa^{-2})} \quad (45)$$

which indicates that in this case the ARF is a function of catchment area and rainfall correlation structure only, and is independent of the particular rainfall regime (i.e. point IDF curves).

How do the ARF values estimated by the proposed method compare to ARFs estimated from actual storms? We carried out such a comparison using

two observed historical storms which occurred in 1913 and 1899, respectively. Fig. 9(a) and (b) present the isohyetal patterns for the two storms. The 1913 storm (reported by Forchheimer, 1913) was a very localized convective event (i.e. a thunderstorm), and produced a maximum of 650 mm of rainfall in 4 h in the Stifting region of Styria, Austria. It was assessed to be a 1000 yr event. The 1899 storm (reported by K. K. Hydrographisches Central-Bureau, 1900) was associated with a long-lasting, synoptic event which covered much of Austria and produced a maximum of 430 mm of rainfall in 96 h in the Erlauf region of Lower Austria. It was assessed to be a 500 yr event.

Fig. 10(a) presents (line with markers) the empirical ARFs estimated for the 1913 storm in the Stifting area using the isohyetal pattern shown in Fig. 9(a). Note that these empirical ARFs are storm-centred ARFs while the proposed method gives fixed-area ARFs. Storm-centred ARFs tend to be slightly smaller than fixed-area ARFs. We then attempted to match these empirical estimates with ARFs estimated by the proposed method (Eq. (44)) through selection of appropriate spatial correlation lengths,  $\lambda$ . This match gave two enveloping spatial correlation lengths:  $\lambda = 1$  and 2 km for the 1913 storm in the Stifting region. In a similar way we evaluated empirical ARFs for the 1899 storm in the Erlauf region and the match with the proposed method gave correlation lengths of  $\lambda = 60$  and 120 km (Fig. 10(b)). These two pairs of spatial correlation lengths correspond well to the observed isohyetal patterns (Fig. 9) and to our present understanding of the physical processes governing rainfall generating mechanisms. In many cases, correlation length  $\lambda$  is a measure of the spatial extent of the rainfall field. The values of  $\lambda$  found here are consistent with the localized convective event (i.e. thunderstorm) of 1913, and the synoptic event of considerable spatial extent of 1899.

While, according to Eq. (44), the ARF is a function of duration  $t_r$ , so far we have not examined in detail the dependence of the ARF on  $t_r$ . Analyses not presented here show that there is only a weak dependence of the ARF on  $t_r$ . In empirical methods  $t_r$  is the major control on the ARF while it is the spatial correlation length  $\lambda$  which is critical in the proposed method. In fact, in empirical methods  $t_r$  is a surrogate for storm type, with convective events having short durations, and synoptic events having longer durations.

We believe that correlation length  $\lambda$  is a more direct and pertinent measure of storm type, and of the governing precipitation processes, and is therefore more relevant than  $t_r$  to the areal reduction of intensity. However,  $\lambda$  and  $t_r$  are often closely related, as is demonstrated in Fig. 10(a) and (b). The 1913 storm in the Stifting region has  $t_r = 4$  hours and  $\lambda = 1\text{--}2$  km, and the 1899 storm in the Erlauf region has  $t_r = 96$  h and  $\lambda = 60\text{--}120$  km. In order for the proposed method to be applied to construct catchment IDF curves we would need to develop consistent relationships between  $\lambda$  and  $t_r$  for the region in question, so that appropriate correlation lengths can be used in the rainfall averaging. This is the only way regional estimates of ARFs can be produced; this is left for further research.

## 7. Conclusions

In this paper, we have presented a new methodology for constructing catchment intensity-duration-frequency (IDF) curves which is based on the spatial correlation structure of rainfall. The methodology consists, in the main, of the areal averaging of the parent rainfall and the transformation of the areally-averaged parent rainfall distribution into the corresponding extreme value distribution according to the theory of Gumbel (1958). To construct catchment IDF curves with the proposed methodology the following pieces of information are needed: (a) point IDF curves for the rainfall regime under study, which follow a Gumbel distribution, i.e. parameters  $b(t_r)$  and  $c(t_r)$ ; (b) the spatial correlation structure of the parent point rainfall process for the storm type considered, i.e.  $\rho_p(r)$  or  $\lambda$ ; and (c) catchment area,  $A$ .

The proposed methodology overcomes the shortcomings of previous work by Rodríguez-Iturbe and Mejia (1974) by distinguishing between the scaling behaviour of the parent and extreme value distributions of the rainfall process. Indeed, the areal reduction factors (ARFs) predicted by Rodríguez-Iturbe and Mejia (1974) are identical to the variance reduction factors  $\kappa^2$  presented in Fig. 2 of this paper while the ARFs for extreme rainfall estimated by the proposed method (Fig. 8) are significantly larger.

The other advantage of the methodology is that with a minimum number of assumptions, the method

reproduces a number of observed properties of extreme areal rainfall. The ARFs estimated by the proposed method were found to decrease with return period, which is consistent with data evidence. Similarly, the coefficient of variation (CV) of rainfall decreases as catchment area increases, which too is consistent with data evidence. We have applied the proposed method to two observed storms in Austria, and found that the correlation lengths of rainfall needed to match empirical ARF estimates were consistent with our understanding of the governing rainfall generation mechanisms.

The main control on catchment IDF curves according to the proposed methodology is the rainfall spatial correlation length,  $\lambda$ , which characterises the storm type. We believe that this is a physically more justifiable measure of storm type than is storm duration,  $t_r$ , which is used in traditional, empirical ARF estimation procedures. However, the spatial correlation length and storm duration are often closely related through the type of storm.

Most of the simplifying assumptions made in this paper have been made for clarity of presentation. These include isotropy, exponential correlogram, exponential/gamma parent distributions, square catchment area, and stationarity. All of these can be easily relaxed, as explained under the respective headings in the paper. As for stationarity, Vanmarcke (1983; p. 226) suggested that the effect of non-stationarity can be represented by including a larger scale component in a nested correlation structure. This has been done in Sivapalan et al. (1990) and Blöschl and Sivapalan (1997b). The most fundamental, though implicit, assumption in the proposed method is that the correlation structure of rainfall does not change with return period; the correlation structure of the parent process has also been used for extreme rainfall. More work is needed to verify or relax this assumption.

This paper has represented an attempt to link approaches used presently in design, based largely on the use of empirically-derived ARFs, with approaches based on some current scientific theories of space–time rainfall fields. In this way we hope to place design practice on a sounder scientific basis, at the same time providing some guidance for new research strategies.

## Acknowledgements

The authors would like to thank the Austrian Science Foundation (FWF), project no. M00298-TEC, for financial support. We thank Dr Mike Hutchinson of the Australian National University and two other anonymous reviewers, and Dr Roman Krzysztofowicz, Editor, for their constructive comments which helped to substantially improve the manuscript.

## Appendix A

The probability density function of  $R$ , the random distance between two independent points in a square of side length  $a$  has been given by Ghosh (1951), and is reproduced below:

$$f_R(r) = \frac{4r}{a^4} \phi(r) \quad (\text{A1})$$

where,

for the range  $r = 0$  to  $r = a$ :

$$\phi(r) = \frac{1}{2} \pi a^2 - 2ar + \frac{1}{2} r^2 \quad (\text{A2})$$

for the range  $r = a$  to  $r = \sqrt{2}a$ :

$$\phi(r) = a^2 \left\{ \sin^{-1} \frac{a}{r} - \cos^{-1} \frac{a}{r} \right\} + 2a \sqrt{r^2 - a^2} - \frac{1}{2} (r^2 + 2a^2) \quad (\text{A3})$$

## References

- Austin, P.M., Houze, R.A. Jr., 1972. Analysis of the structure of precipitation patterns in New England, *J. Appl. Meteorol.*, 11, 926–934.
- Bacchi, B., Ranzi, R., 1996. On the derivation of the areal reduction factor of storms, *Atmos. Research*, 42, 123–135.
- Bell, F.C., The areal reduction factors in rainfall frequency estimation. Natural Environment Research Council (NERC) Report No. 35, Institute of Hydrology, Wallingford, U.K., 1976.
- Benjamin, J. R., Cornell, C. A., Probability, Statistics and Decision for Civil Engineers, McGraw-Hill, New York, 684p., 1970.
- Berndtsson, R., Spatial hydrological processes in a water resources planning perspective—An investigation of rainfall and infiltration in Tunisia, Report No. 1009, Dept. of Water Resour. Eng., Inst. of Technology, University of Lund, Lund, Sweden, 315p., 1988.
- Blöschl, G., Sivapalan, M., 1995. Scale issues in hydrological modelling—a review, *Hydrol. Process.*, 9, 251–290.
- Blöschl, G., Sivapalan, M., Process controls on flood frequency, 2, Storm properties, runoff generation and the return period. *Water Resour. Res.*, (submitted).
- Blöschl, G., Sivapalan, M., Process controls on regional flood frequency: Coefficient of variation and basin scale. *Water Resour. Res.*, 33(12), 2967–2980, 1997b.
- Blöschl, G., Gutknecht, D., Watzinger, A., Ermittlung eines Bemessungshochwassers für die Sperre Erlaufklause (Design flood for the Erlaufklause dam), Tech. Report, Inst. f. Hydraulik, Technical University of Vienna, 1995.
- Chow, V. T., Maidment, D. R., Mays, L. W., Applied Hydrology, McGraw-Hill, 1988.
- Dalrymple, T., Flood frequency methods, U. S. Geol. Surv. Water Supply Pap. 1543-A, 11-51, 1960.
- Eagleson, P. S., Dynamic Hydrology, McGraw-Hill, New York, 462p., 1970.
- Eagleson, P.S., 1972. Dynamics of flood frequency, *Water Resour. Res.*, 8 (4), 878–898.
- Eagleson, P.S., Qinliang, W., 1985. Moments of catchment storm area, *Water Resour. Res.*, 21 (8), 1185–1194.
- Forchheimer, Ph., Der Wolkenbruch im Grazer Hügelland vom 16. Juli 1913. Sitzungsberichte Österr. Akad. Wiss., Math.-naturwiss. Kl. Sitzungsber. Bd. CXXII, Abt., 2A, 1913, pp. 2099–2109.
- Foufoula-Georgiou, E., Georgakakos, K. P., Recent advances in space-time precipitation modeling and forecasting, in: Recent Advances in the Modeling of Hydrologic Systems, D. S. Bowles and P. E. O'Connell (eds.), D. Reidel Publ., Boston, Mass., 1991.
- Ghosh, B., 1951. Random distances within a rectangle and between two rectangles, *Bull. Calcutta Math. Soc.*, 43, 17–24.
- Grebner, D., Klimatologie und Regionalisierung starker Gebietsniederschläge in der nordalpinen Schweiz, Zürcher Geographische Schriften, Heft 59, Geographisches Institut, ETH Zürich, 1995.
- Gumbel, E. J., Statistics of Extremes, Columbia Univ. Press, New York, 1958.
- Gupta, V.K., Dawdy, D.R., 1995. Physical interpretations of regional variations in the scaling exponents of flood quantiles, *Hydrol. Process.*, 9, 347–361.
- Gutknecht, D., Ein Computermodell zur Erzeugung einer Folge von Regenereignissen, Tech. Report, Inst. f. Hydraulik, Technical University of Vienna, 1977.
- Hobson, C., Wood, E. F., A study of scale effects in flood frequency response, in: Scale Problems in Hydrology, I. Rodriguez-Iturbe, V. K. Gupta and E. F. Wood (eds.), pp. 133–158, D. Reidel Publ., Hingham, Mass., 1986.
- Hobbs, P.V., Locatelli, J.D., 1978. Rainbands, precipitation cores and generating cells in a cyclonic storm, *J. Atmos. Sci.*, 35, 230–241.
- K. K. Hydrographisches Central-Bureau, Die Hochwasserkatastrophe des Jahres 1899 im Österreichischen Donaugebiete. Beiträge zur Hydrographie Österreichs, IV. Heft. Braumüller, Wien, 1900.
- Myers, V. A., Zehr, R. M., A methodology for point-to-area rainfall frequency ratios, NOAA Tech. Report NWS 24, Washington, D.C., 1980.

- Omolayo, A.S., 1993. On the transposition of areal reduction factors for rainfall frequency estimation, *J. Hydrol.*, 145, 191–205.
- Pilgrim, D. H. (Editor), *Australian Rainfall and Runoff: A Guide to Flood Estimation*, 3rd Edition, Vol. 1. Institution of Engineers Australia, Canberra, A.C.T., 1987.
- Rodríguez-Iturbe, I., Mejia, J.M., 1974. On the transformation from point rainfall to areal rainfall, *Water Resour. Res.*, 10 (4), 729–735.
- Schimpf, H., 1970. Untersuchungen über das Auftreten beachlichter Niederschläge in Österreich, *Österreichische Wasserwirtschaft*, 22, 121–127.
- Sivapalan, M., *Scale Problems in Rainfall, Infiltration and Runoff Production*, PhD dissertation, Dept. of Civil Engrg., Princeton University, 271 p., 1986.
- Sivapalan, M., Hoeg, S., Woods, R. A., On space–time averaging of rainfall by catchments: A new geometrical framework, *Proceedings of the 4th International Workshop on Scale Problems in Hydrology*, G. Blöschl, M. Sivapalan, V. K. Gupta and K. J. Beven (eds.), Inst. f. Hydraulik, Technical University of Vienna, Austria, p. 17, 1996.
- Sivapalan, M., Blöschl, G., D. Gutknecht, Process controls on flood frequency. 1. Derived flood frequency, *Water Resour. Res.*, (submitted).
- Sivapalan, M., Beven, K.J., Wood, E.F., 1990. On hydrologic similarity, 3, A dimensionless flood frequency model using a generalised geomorphic unit hydrograph and partial area runoff generation, *Water Resour. Res.*, 26 (1), 43–58.
- Sivapalan, M., Wood, E.F., 1987. A multidimensional model of non-stationary space–time rainfall at the catchment scale, *Water Resour. Res.*, 23 (7), 1289–1299.
- Smith, J.A., 1992. Representation of basin scale in flood peak distributions, *Water Resour. Res.*, 28, 2993–2999.
- Srikanthan, R., A Review of the Methods for Estimating Areal Reduction Factors for Design Rainfalls, Report 95/3, Cooperative Research Centre for Catchment Hydrology, Melbourne, Australia, 36p., 1995.
- U. S. Weather Bureau, Rainfall intensity-frequency regime. 1. The Ohio Valley; 2. Southeastern United States. Tech. Paper No. 29, U. S. Dept. of Commerce, Washington, D.C., 1957.
- Vanmarcke, E., *Random Fields: Analysis and Synthesis*, MIT Press, Cambridge, Mass., 382p., 1983.
- Warrilow, D. A., Sangster, A. B., Slingo, A., Modelling of land surface processes and their influence on European climate, *Dyn. Climatol. Tech. Note DCTN 38*, U.K. Meteorological Office, Bracknell, 92p., 1986.
- Waymire, E., Gupta, V.K., Rodríguez-Iturbe, I., 1984. A spectral theory of rainfall intensity at the meso-b scale, *Water Resour. Res.*, 20 (10), 1453–1465.
- Wood, E.F., Hebson, C.S., 1986. On hydrologic similarity. 1. Derivation of the dimensionless flood frequency curve, *Water Resour. Res.*, 22 (11), 1549–1554.
- Zawadzki, I., 1973. Statistical properties of precipitation patterns, *J. Appl. Meteorol.*, 12, 459–472.